Regular Article

PHYSICAL CHEMISTRY RESEARCH
Published by the
Iranian Chemical Society
www.physchemres.org
info@physchemres.org

Phys. Chem. Res., Vol. 8, No. 3, 511-527, September 2020
DOI: 10.22036/pcr.2020.213588.1714

TD-DFT, NBO, AIM, RDG and Thermodynamic Studies of Interactions of 5-Fluorouracil Drug with Pristine and P-doped Al12N12 Nanocage

M. Rezaei-Sameti* and H. Zanganeh

Department of Applied Chemistry, Faculty of Science, Malayer University, Malayer, 65174, Iran

(Received 18 December 2019, Accepted 16 May 2020)

In the present study, the capability of the pristine and P-doped Al12N12 nanocage to deliver and detect of 5-Fluorouracil (5-FU) anticancer drug is investigated using the density functional theory (DFT) at the cam-B3LYP/6-31G(d,P) level of theory. The adsorption energy, thermodynamic parameters, natural bond orbital (NBO), atom in molecule theory (AIM), quantum parameters, reduced density gradient (RDG) and UV-Vis spectrum for all selected models are calculated and results are analyzed. The values of adsorption energy (E_{ads}) and thermodynamic parameters (ΔG and ΔH) for 5-FU@Al12N12 and 5-FU@Al12N11P complexes are negative and obtained results reveal that all adsorption processes are spontaneous and suitable to make a delivery of drug. The $\Delta\Delta G_{(sol)}$ values of the all systems understudy in the presence of water and ethanol solvents are positive and this property is favourable to shooting drug in biological system. The AIM, RDG, NBO results indicate that the interaction between 5-FU drug and Al12N12 nanocage is weak covalent or strong electrostatic type. The band gap energy of the 5-FU/Al12N12 nanocage complex alters slightly from original values, indicating that pristine and P doped Al12N12 nanocage are not excellent candidates for making a sensitive sensor for the 5-FU drug.

Keywords: Al12N12, P-doped, 5- Fluorouracil drug, Density functional theory, RDG, AIM

INTTRODUCTION

In the last decade, the extensive studies have been performed on various nanoparticles such as nanotubes, nanocages, and nanowires from III and V group table due to their numerous electrical, mechanical, and technological applications in nanoengineering, nanoelectronic devices and nano compounds design [1-2]. Aluminum nitride nano structures with high-temperature stability, high hardness, high thermal conductivity, low thermal expansion, semiconductor properties, specific physical and chemical properties are suitable for electronic applications and making a sensor or adsorbent for various toxic materials and drug compounds [3-13]. In the last decades, many researchers have focused on the synthesis, characterization and structural properties of AlN nanotubes, nanocages, nanosheets, and nanowires. Among of (AlN)n nanocages, Al12N12 is the most stable structure [14-18]. In the recent years, the potential of pristine and doped Al12N12 for adsorbing and detecting various compounds such as Tabun[19], dehydrogenation of formic acid [20], sulfur mustard [21], Cl_2 [22], cyanogen gas [23], acetylene and ethylene molecules [24], H_2 [25], adenine, uracil, cytosine [26], guanine [27], hydrogen storage [28], fluorinated [29], phosgene [30], NH_3 [31], acetone [32], NO_2 and SO_2 [33], pyrrole [34], and H_2O_2 [35] has been investigated with theoretical methods. Based on the results, the pristine and doped models of Al12N12 could be the excellent adsorbents or sensors for the compounds aforementioned in environmental systems.

With advancement in drug production and drug delivery in biological systems, the extensive research activities have been performed on optimizing the efficiency of drug therapy in human body. One of the most practical methods for this purpose is using nanomaterial for the delivery of drug in human body. The 5-Fluorouracil (5-FU) drug is

*Corresponding author. E-mail: mrsameti@malayeru.ac.ir

widely used to remedy the cancer of lung, colon, skin, stomach, lung, gastrointestinal, and breast [36-38]. The biological half-life and selectivity of 5-FU are very short, so, many novel nanomaterial carriers such as silica nanoparticles, chitosan nanoparticles, cationic cyclodextrin/ alginate, nanogels, and magnetic nanoparticles have been proposed to control the release of 5-FU drug in biological systems [39-46]. Vatanparast *et al.*'s [47] results revealed that the doped graphene with Al&N and Al&P atoms were suitable for 5-FU delivery in biological systems. The results obtained by Hadipour *et al.* indicated that doping B, Si and Al atoms improves the drug delivery properties of C60 [48]. Shayan *et al.*'s results showed that the encapsulation of the 5-FU molecule on the surface of BNNTs was more stable than the hybrid complexes [49].

Following our previous study [50-55], in this work, we investigate the adsorption and interaction of 5-FU molecule on the surface of the pristine and P-doped Al12N12 nanocage using the DFT and TD-DFT methods. The geometrical parameters, adsorption energy, thermodynamic and quantum parameters, the topological parameters of AIM, the NBO, RDG, DOS plots and UV-Vis spectrum for all selected models are calculated. The results of this work can be useful for making a drug delivery tool or a drug sensor in biological systems.

COMPUTATIONAL DETAILS

In this work, we considered different possible positions for adsorption of 5-FU drug on the surface of pristine and P-doped Al12N12 nanocage, and then, four possible configurations were selected for this research (see Fig. 1). According to the structure of the 5-FU drug, it was observed that among all the situations, the four selected positions were both structurally and energetically efficient.

The labels A and C denote the pristine and P-doped Al12N12 nanocages, respectively. The a, b, c and d indexes (see Fig. 1) denote the orientation of 5-FU drug adsorption on the surface of AlN nanocage. The A-a to C-d models are optimized using DFT method at the cam-B3LYP/6-31G(d,p) level of theory [56] with performing the GAMESS suite of programs [57]. The adsorption energy, deformation energy, and thermodynamic parameters (such as Gibbs free energy (G), enthalpy (H) and entropy(S)) for the interaction of 5-FU with the pristine and P-doped Al12N12 nanocage are calculated by Eqs. (1)-(4):

$$E_{ads} = E_{5-FU/Al12N12} - (E_{5-FU} + E_{Al12N12}) \quad (1)$$

$$\Delta M = M_{5-FU/Al12N12} - (M_{5-FU} + M_{Al12N12}) \qquad M: H, S, G \quad (2)$$

$$E_{def} = E - E^{*} \quad (3)$$

$E_{5-FU/Al12N12}$ *and* $M_{5-FU/Al12N12}$ are the total energy and thermodynamic parameters of the 5-FU/Al12N12 complex, respectively. E_{5-FU} *and* M_{5-FU} are the total energy and thermodynamic parameters of pure 5-FU, respectively, and $E_{Al12N12}$ *and* $M_{Al12N12}$ are the total energy and thermodynamic parameters of pristine or P doped Al12N12 nanocage, respectively. In Eq. (3), E is the total energy of pure Al12N12 or 5-FU drug, and E^{*} is the total energy of Al12N12 in the presence of 5-FU or the total energy of 5-FU in the presence of Al12N12 nanocage.

$$\Delta\Delta G_{(sol)} = \Delta G_{5-FU/Al12N12(sol)} - (\Delta G_{5-FU(sol)} + \Delta G_{Al12N12(sol)}) \quad (4)$$

In Eq. (4), $\Delta G_{5-FU/Al12N12(sol)}$, ΔG_{5-FU} and $\Delta G_{Al12N12(sol)}$ are the changes of Gibbs free energy 5-FU/Al12N12 complex, 5-FU and Al12N12 nanocage in solvent (water, ethanol) phase, respectively.

The highest occupied molecular orbital (HOMO) and lowest unoccupied molecular orbital (LUMO) energies, the band gap energy (E_g), the electrochemical potential (μ), global hardness (η), and charge transfer parameters (ΔN) were calculated for all the systems understudy by Eqs. (5)-(8) [50-55]

$$E_{gap} = E_{LUMO} - E_{HOMO} \quad (5)$$

$$\mu = (E_{HOMO} + E_{LUMO})/2 \quad (6)$$

$$\eta = (E_{LUMO} - E_{HOMO})/2 \quad (7)$$

$$\Delta N = -(E_{HOMO} + E_{LUMO})/(E_{LUMO} - E_{HOMO}) \quad (8)$$

RESULTS AND DISCUSSION

Structures, Adsorption Energies, and Thermodynamic Parameters

The optimized structures of the A-a to C-d adsorption models are shown in Fig. 2. In optimized structures, the Al-N bond length, Al-N-Al bond angles of Al12N12 nanocage

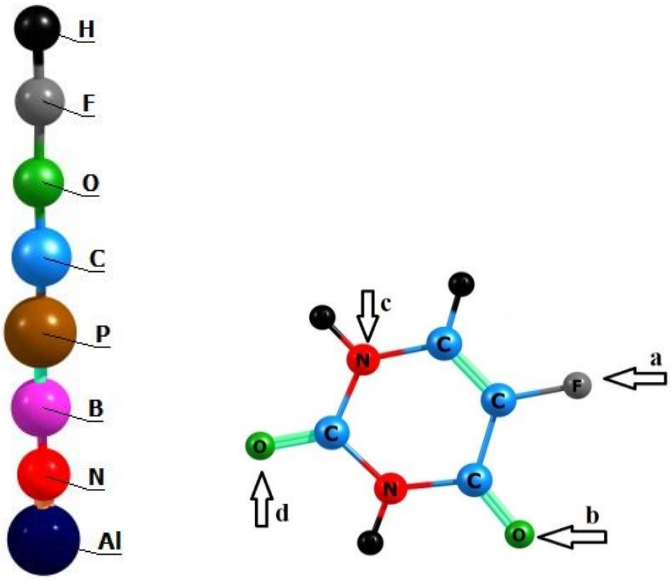

Fig. 1. The optimized structures of 5-Fluorouracil drug and corresponding adsorption positions, a, b, c and d.

and its bond distances, and the bond angle between 5-FU and nanocage are shown in Fig. S1 and Fig. 2, respectively. According to the results, the average bond length Al-N in Al12N12 nanocage is 1.85 Å and with doping P atom the Al-N bond length increased significantly from 1.85 to 2.37 Å. This result is in agreement with the literature [18-30]. The bond angle <Al-N-Al in the pristine model is 112.57º and with doping P atom bond angle <Al-P-Al reduces significantly to 87.81º, because the radius of P atom is larger than N atom. With adsorbing 5-FU drugs on the surface of nanocage the structural properties (Al-N bond length and Al-N-Al bond angle) of system change slightly from the pristine model. According to the calculated structural results, the bond distance between 5-FU and AlN nanocage in the A-a, A-c, A-d, C-a, C-c and C-d models are 2.04, 2.25, 1.90, 2.07, 1.90 and 1.92 Å, respectively.

The bond angle between 5-FU drug and AlN nanocage is in the range of 102.41 to 111.13º. By using optimized structures, the adsorption and deformation energy for adsorbing 5-FU on the pristine and P doped Al12N12 nanocage are computed, and the calculated results are given in Table 1. Based on the calculated results, the values of adsorption energy for all studied systems are negative, and the adsorption process is exothermic. The adsorption energy of the system depends on the orientation of 5-FU drug adsorption and doping atom. The values of adsorption energy for the A-a, A-c and A-d adsorption model are -14.64, -7.87 and -39.10 Kcal mol^{-1}, respectively, and for the C-a, C-c and C-d models are -12.07, -38.16 and -35.37 Kcal mol^{-1}, respectively. In the pristine model, the adsorption of 5-FU from **d** orientation and in the P doped from **c** orientation is more stable than other models. The deformation energy values of AlN nanocage and 5-FU drug (see Table 1) are negative, indicating that the significant curvature in the geometry of nanocage and 5-FU drug occurs after the adsorbing process.

On the other hand, the absolute values of deformation energy of drug and nanocage in the A-d and C-c models are more than those in other models studied. It is notable that in the A-d and C-c models, the structure of nanocage and 5-FU drug changes significantly from original states. The dipole moments of the A-a, A-c, A-d, C-a, C-c and C-d models are -4.32, -4.30, -4.06, -4.37, -4.30 and -4.08 Debye, respectively. Inspection of results indicates that the adsorption of the 5-FU drug from the a orientation (F site) has the most dipole moment and from d orientation (O site) has the lowest dipole moment and this property is important to determine the polarity of compound.

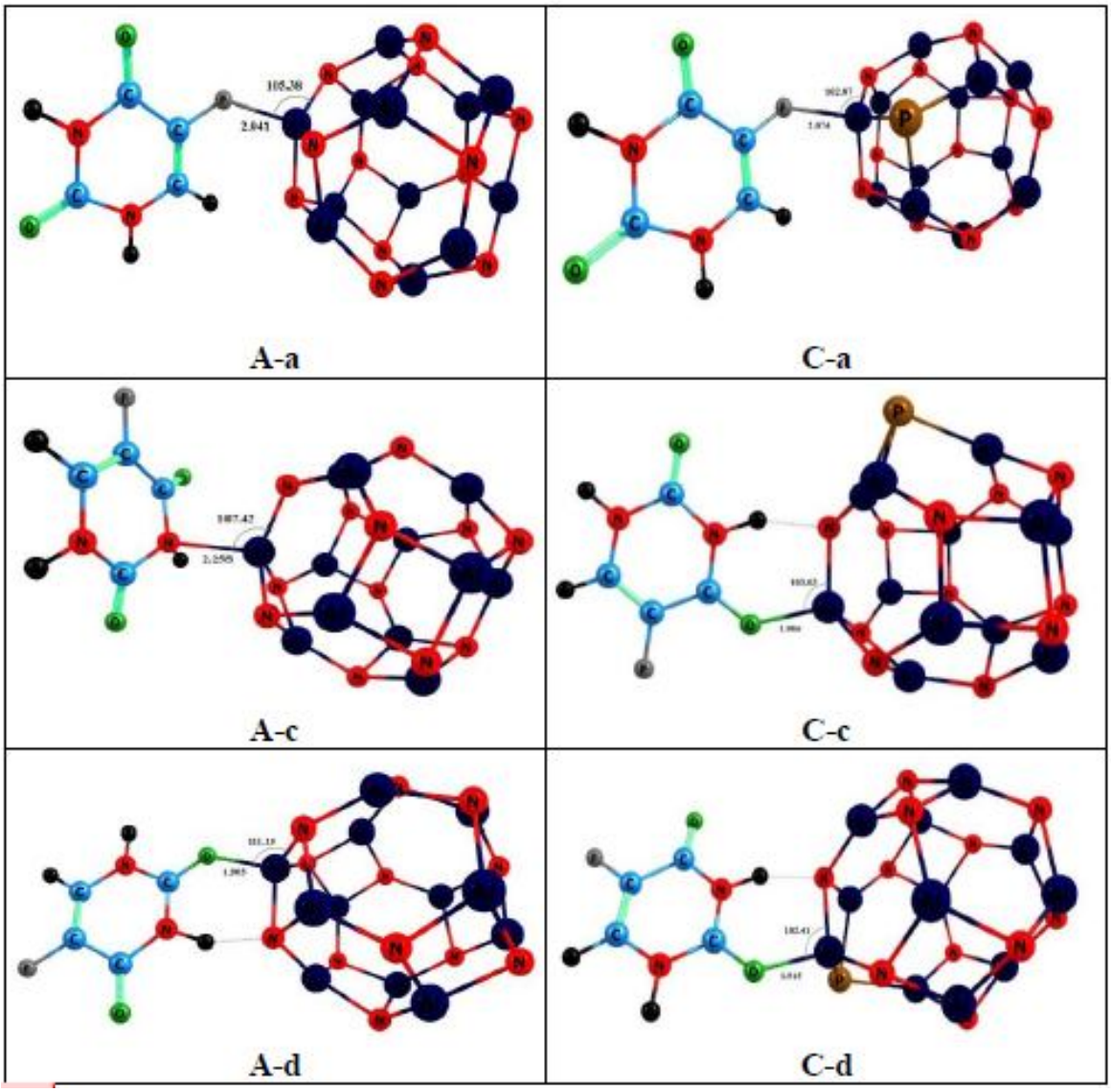

Fig. 2. 2D views of 5-Fluorouracil drug adsorption on the surface of Al12N12 nanocage at the A-a to C-d models.

The NBO charge density of 5-FU drug for all adsorption models is positive. The positive values of charge density indicate that the electron charge transfer occurs from the 5-FU drug toward the nanocage surface.

To investigate the adsorption of the 5-FU drug on the surface of nanocage, the thermodynamic parameters in the gas and solvent (water and ethanol) phases are computed by Eq. (4) and results are given in Table 1. Based on the calculated results, the changes of enthalpy, entropy and Gibbs free energy values for the A-a, A-c, A-d, C-a, C-c and C-d models are negative. Negative values of enthalpy change and Gibbs free energy indicate that the adsorption process between 5-FU and AlN nanocage is exothermic and spontaneous. A comparison of the thermodynamic results exhibits that the values of ΔG, ΔH and ΔS of A-d model (in the pristine Al12N12) and C-c model (in P doped Al12N12) are more than those in other models and these results have a good agreement with adsorption energies. These results

Table 1. Adsorption Energy (E_{ads}), Deformation Energy of 5-Fluorouracil ($E_{def\,(5\text{-}FU)}$), Al12N12 ($E_{def(nano)}$), Complex Al12N12/5-FU, Binding Energy E_{bin}, Thermodynamic Parameters and Dipole Moment of Al12N12/5-FU Complex and Al12N11P/5-FU Complex for A-a to C-d Models. Energies are in kcal mol^{-1}

Property	A-a	A-c	A-d	C-a	C-c	C-d
E_{ads}	-14.64	-7.87	-39.10	-12.07	-38.16	-35.37
$E_{def(nano)}$	-1.45	-1.12	-5.71	-1.46	-5.45	-5.31
$E_{def(5\text{-}FU)}$	-1.61	-4.74	-6.40	-1.51	-5.22	-5.21
d/Debye	-4.32	-4.30	-4.06	-4.37	-4.30	-4.08
ρ_{NBO}	0.10	0.10	0.07	0.09	0.08	0.08
ΔG	-24.46	-17.76	-26.11	-0.24	-25.03	-22.31
ΔH	-13.57	-6.80	-51.29	-11.07	-37.54	-34.70
ΔS	-36.84	-36.77	-42.25	-36.10	-42.10	-41.58
$\Delta\Delta G_{(sol)water}$	1.78	1.68	0.89	1.11	0.26	0.04
$\Delta\Delta G_{(sol)ethanol}$	2.69	2.78	3.09	3.17	3.49	3.43

demonstrate that the pristine and P doped Al12N12 nanocages probably can be used for the drug delivery in the biological systems. On the other hand, this result confirms that the adsorption of 5-FU from d orientation (O site) of pristine nanocage and c orientation (N site) of P doped nanocage is more favorable than that in other sites. The trend of absolute thermodynamic values in the pristine and P doped Al12N12 models are in order: A-d > A-a > A-c and C-c > C-d > C-a, respectively. The changes of Gibbs free energy ($\Delta\Delta G(sol)$) for adsorption of the 5-FU drug on the surface of AlN nanocage in the water and ethanol solvents are calculated by Eq. (4), the calculated results are listed in Table 1. Comparison results reveal that the $\Delta\Delta G(sol)$ values for all studied systems are positive. The positive value of $\Delta\Delta G(sol)$ indicates that the adsorption process in the presence of solvent is unspontaneous, and dissociation drug occurs in the solvent phase. This property is probably suitable for drug delivery in the biological systems. Interestingly, the A-d and C-c models with the highest absorption energy in the gas phase have the highest positive amount of $\Delta\Delta G(sol)$ in ethanol solution. Therefore, these models are more suitable for the absorption of the drug in the gas phase and release it in an ethanol solvent. This feature is probably beneficial in terms of biological and drug treatment in the human body.

Electrical Properties and Quantum Parameters

To investigate the reactivity and electrical properties of nanocage, the HOMO and LUMO orbitals are calculated. The calculated HOMO and LUMO orbital results are shown in Fig. 3. According to the calculated results, the HOMO orbital density in the A-a, A-c, A-d, C-a, C-c and C-d models are distributed around nanocage. The LUMO orbital density of the A-a, A-d and C-a models are distributed around nanocage, whereas in the A-c, C-c and C-d models the LUMO orbital density is localized around 5-FU drug surface. This result reveals that in the A-c, C-c and C-d models the surface of the 5-FU drug is suitable for nucleophilic species, whereas the surface of AlN nanocage for all studied systems is favorable for electrophilic species

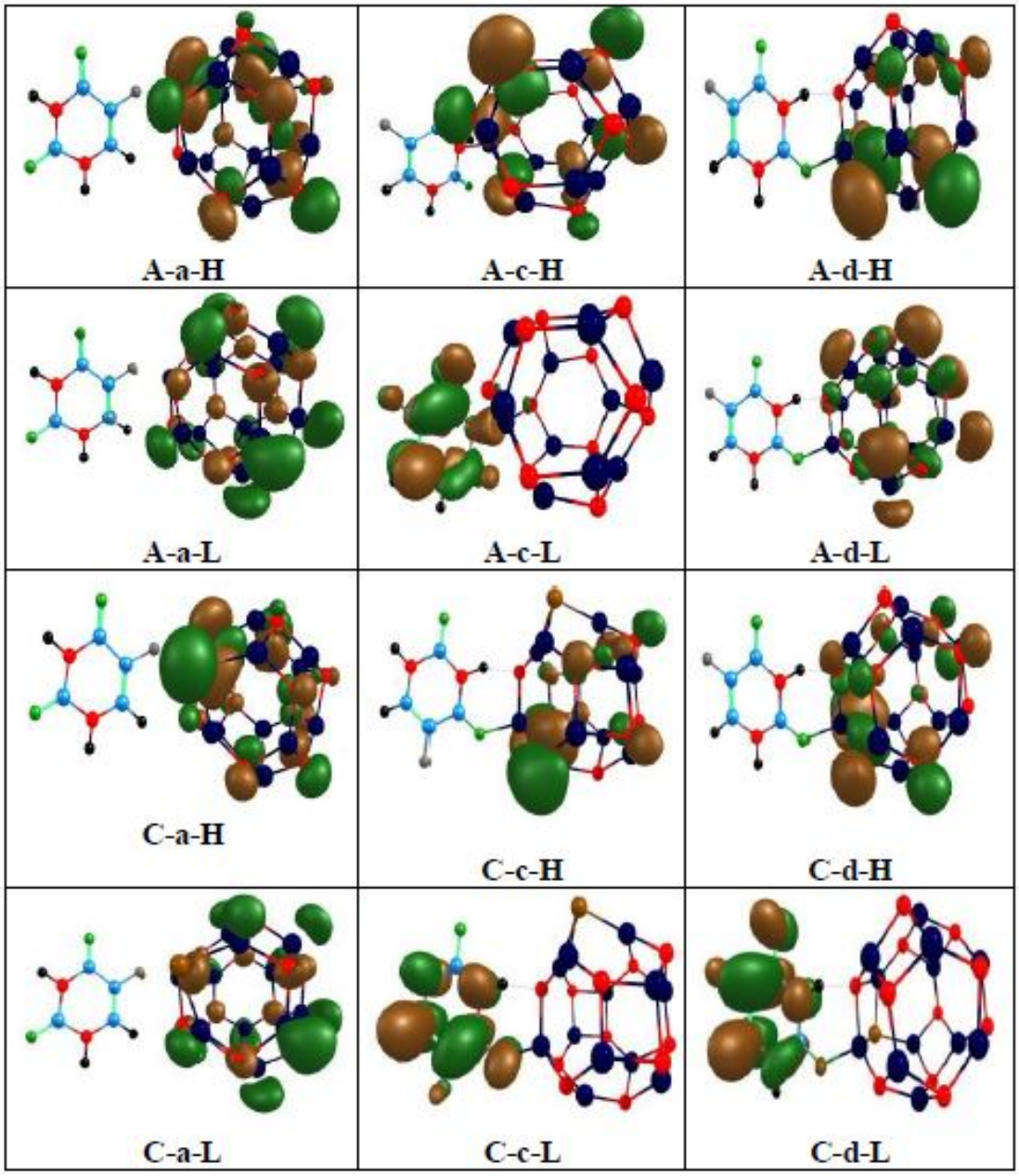

Fig. 3. Plots of HOMO and LUMO orbital structures for 5-Fluorouracil drug adsorption on the surface of Al12N12 nanocage at the A-a to C-d models.

attack.

From using the HOMO and LUMO energy, the band gap, global hardness, chemical potential (μ) and charge transfer parameters (ΔN) for all studied systems are calculated and results are listed in Table 2. The bandgap energy between HOMO and LUMO is in the range of 3.31-3.98 eV. This result indicates that 5-FU drug adsorption is accompanied a slight change in band gap energy and so, the pristine and P doped AlN nanocage will not be sensitive sensors for the 5-FU drug in the biological

Table 2. Quantum Parameters for Adsorption of 5-Fluorouracil (5-FU) on the Surface of Pristine (A Model) and P (C Model) Doped Al12N12 for A-a to C-d Models. The Values are in eV

Model	A-a	A-c	A-d	C-a	C-c	C-d
E_{HOMO}	-6.27	-6.17	-5.98	-6.36	-5.95	-6.01
E_{LUMO}	-2.37	-2.42	-2.14	-2.37	-2.65	-2.14
E_{gap}	3.91	3.75	3.84	3.98	3.31	3.87
η	1.95	1.88	1.92	1.99	1.65	1.94
μ	-4.32	-4.30	-4.06	-4.37	-4.30	-4.08
ΔN	2.21	2.29	2.12	2.19	2.60	2.10

systems.

The global hardness and electrochemical potential of all studied systems are in the range of 1.65-1.99 eV and -4.06 to -4.37 eV, respectively. With adsorption of 5-FU, the reactivity of AlN nanocage increases significantly from the original values. This property is favorable for deliver and attachment the 5-FU drug to the objective position of the biological system. On the other hand, the charge transfer parameters (ΔN) values for all studied systems are in the range of 2.10-2.60. The positive values of ΔN indicate that the electron charge transfer occurs from 5-FU toward the nanocage surface, so, the electron density around nanocage increases. The density of state (DOS) and partial density of state (PDOS) plots for all systems are shown in Fig. 4 and Fig S5, respectively.

The DOS plots of the A-a, A-c, A-d, C-a, C-c and C-d reveal that the number and altitude of peaks in all plots are the same (see Fig. 4).

The band gap energy between HOMO and LUMO in all models alter slightly from original values, and so, the conductivity of nanocage remains almost constant. This result confirms that the pristine and P doped AlN nanocage is unfavorable for making a sensitive sensor for detecting 5-FU drug. According to PDOS plots (Fig. S5), in the A-a, A-c and A-d models, the interactions of 2P orbitals of F, N and O atoms of 5-FU drug with 2P orbitals of Al and N atoms of Al12N12 nanocage in the HOMO region are stronger than those in other orbitals. Whereas, in the LUMO region, the interaction of 3P orbital of F atom of 5-FU, with 3P orbital of Al and N atoms of AlN nanocage, is more considerable. In the C-a, C-c and C-d model, the overlap of 2P orbitals of F, N, O and C atoms of 5-FU with 2P orbitals of Al, N and P atoms of AlN nanocage is more than the other orbitals. In the LUMO region, the interaction of 3P orbitals of F, O and C atoms of 5-FU drug with 3P orbitals of Al, N and P atoms of AlN nanocage is more evident.

Interestingly, these interactions in the A-c and C-c models are more remarkable than those in other models. On the other hand, the altitude of PDOS peaks of 2P and 3P orbitals of Al, N, O, F atoms is larger than that in other atoms.

Quantum Theory of Atoms in Molecules (QTAIM)

To understand the nature of interactions between 5-FU drugs with pristine and P doped AlN nanocage, the QTAIM parameters [58] at the bond critical point (BCP) between drug and AlN nanocage are calculated using the Multiwfn software. The total electronic densities (ρ) and Laplacian of electron densities ($\nabla^2\rho$), the potential energy (V_{BCP}), the total electronic energy (H_{BCP}), the kinetic energy (G_{BCP}) are determined for all the systems understudy and the calculated results are given in Table 3. The bond critical point of interaction between 5-FU drug with AlN nanocage for all systems is shown in Fig. 5.

The calculated results indicate that the values of $\nabla^2\rho$ and H_{BCP} for all the systems are positive. The positive

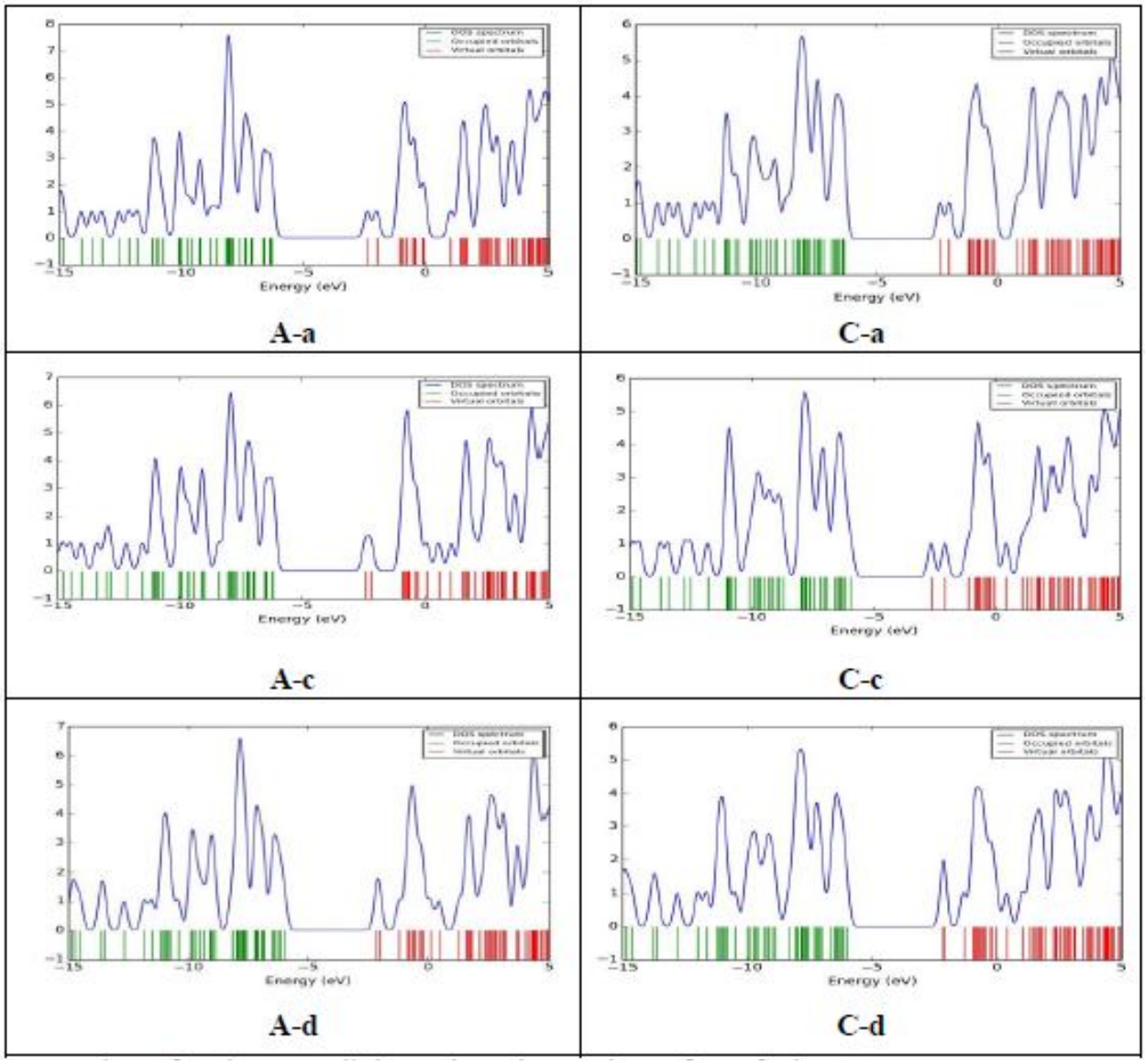

Fig. 4. The DOS Plots of 5-Fluorouracil drug adsorption on the surface of Al12N12 nanocage at the A-a to C-d models.

values of $\nabla^2\rho$ and H_{BCP} detonate that the interaction between 5-FU and nanocage is a weak covalent or a strong electrostatic. The |V(r)|/G(r) ratio is used to determine the strength of the interaction between drug and nanocage. According to QTAIM theory, $|V|/G < 1$ is related to weak interactions and $|V|/G > 2$ is related to strong interactions between drug and nanocage. Comparison the results reveal that the ratio |V(r)|/G(r) for all systems is smaller than 1 and for the A-c model is larger than 2. So, the interaction between 5-FU drug and AlN nanocage in the A-c is stronger than that in other models.

Noncovalent Interaction (NCI)

The noncovalent interaction method is used to further understand the weak interactions between 5-FU drug with the pristine and P doped AlN nanocage using the Multiwfn

Table 3. The Topological Parameters of QAIM Method for A-a to C-d Adsorption Models

	A-a	A-c	A-d	C-a	C-c	C-d
ρ	0.0328	0.0312	0.0557	0.0308	0.0558	0.0544
$\nabla^2\rho$	0.1977	0.1191	0.3933	0.1711	0.3904	0.3783
V(r)	-0.0451	-0.0334	-0.0826	-0.0410	-0.0083	-0.0798
G(r)	0.0473	0.0136	0.0904	0.0419	0.0901	0.0872
|V(r)|/G(r)	0.9535	2.4559	0.9137	0.9797	0.0921	0.9151
H(r)	0.0022	-0.0018	0.0078	0.0009	0.0075	0.0074

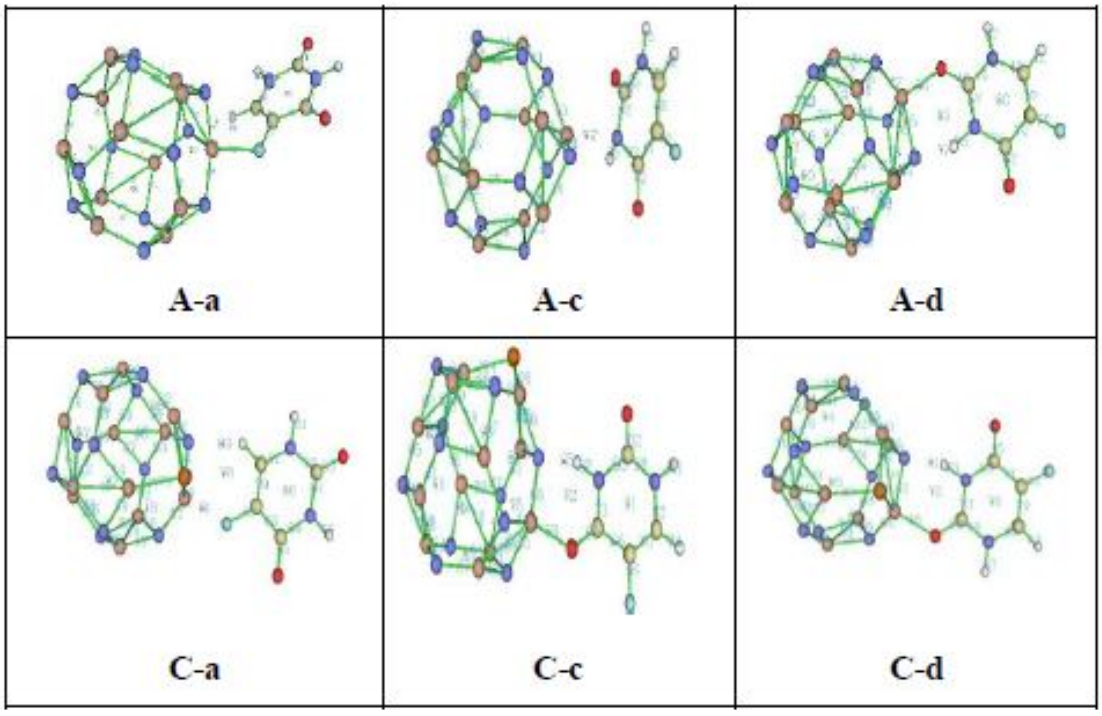

Fig. 5. The bond critical point of interaction between 5-FU drug with Al12N12 nanocage at the A-a to C-d models.

software.

In this method, the reduced density gradient (RDG) [59-60] at low densities is calculated by:

$$RDG(r) = \frac{1}{2(3\pi^2)^{1/3}} \frac{|\nabla\rho(r)|}{\rho(r)^{4/3}} \quad (9)$$

The noncovalent interactions between the two compounds are determined by the small values of RDG.

The sign(λ_2)ρ(r) (product between electron density ρ(r) and the sign of hessian matrix (λ_2)) is used to determine the different types of interactions. In these scatter graphs, the X-axis and Y-axis are sign((λ_2)ρ(r)) and RDG function,

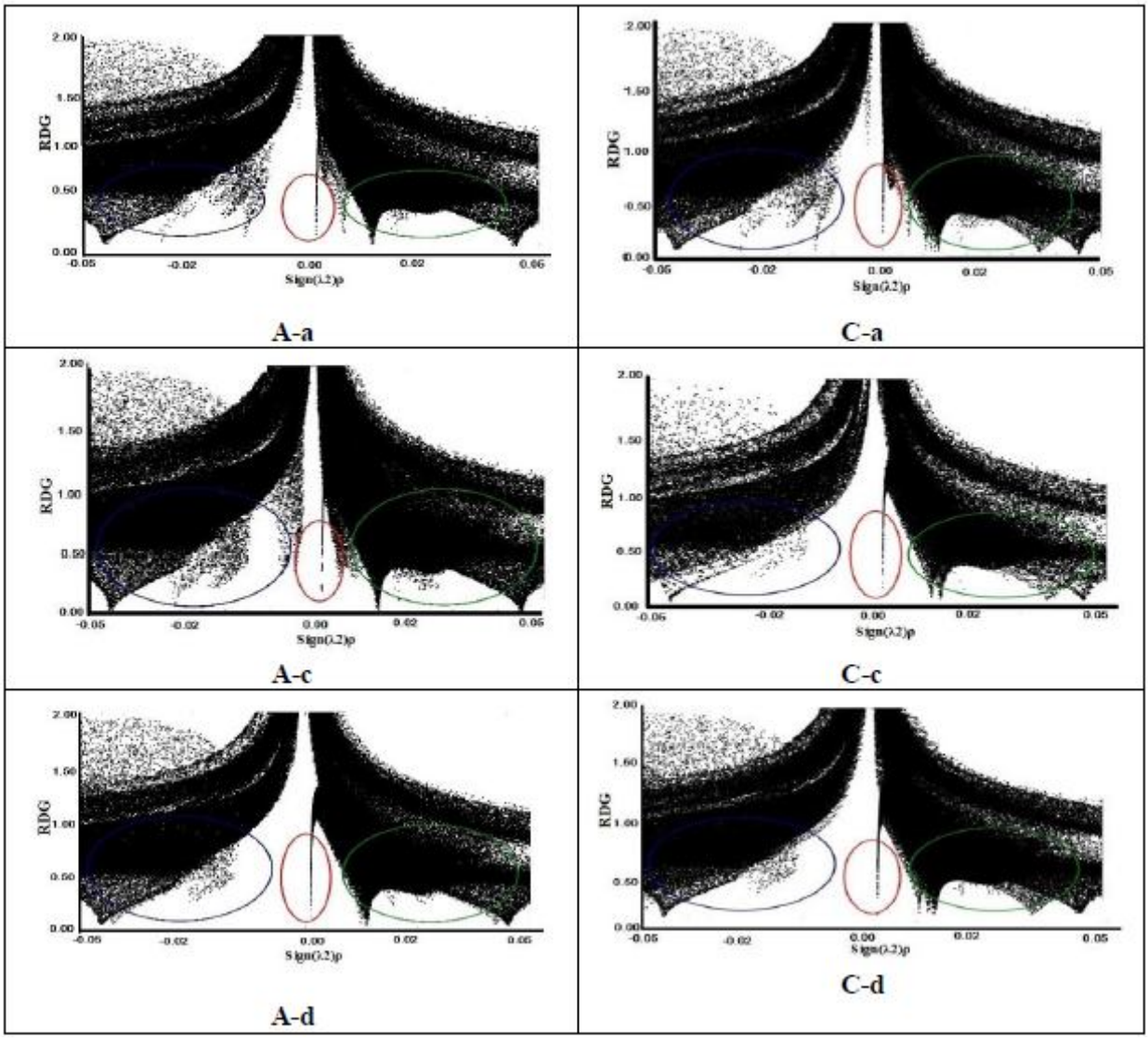

Fig. 6. The RDG plots of interaction between 5-FU drug with Al12N12 nanocage at the A-a to C-d models.

respectively. According to these scatter graphs, the $sign(\lambda_2)\rho < 0$, $sign(\lambda_2)\rho > 0$ and $sign(\lambda_2)\rho \approx 0$ represent the attractive interaction (H-bonding), repulsion interaction, and the van der Waals (vdW) interaction, respectively. The calculated RDG scatter graphs for all the systems are shown in Fig. 6. The blue, red and green circle represent the attractive, vdW and repulsive interactions, respectively. Inspection of results in Fig. 6 reveals that the RDG distribution for all the systems is localized in the $sign(\lambda_2)\rho < 0$ (blue) region and it reveals that the interaction between 5-FU drug and the pristine and P doped AlN nanocage is an attractive interaction type. The attractive interaction caused the 5-FU drug is bonded to the surface of nanocage and it can be carried to the target site of the drug in the body. On the other hand, the attractive interaction between 5-FU with AlN nanocage in the A-c model is more than other states and these models are more suitable for making deliveries and carriers of the 5-FU drug.

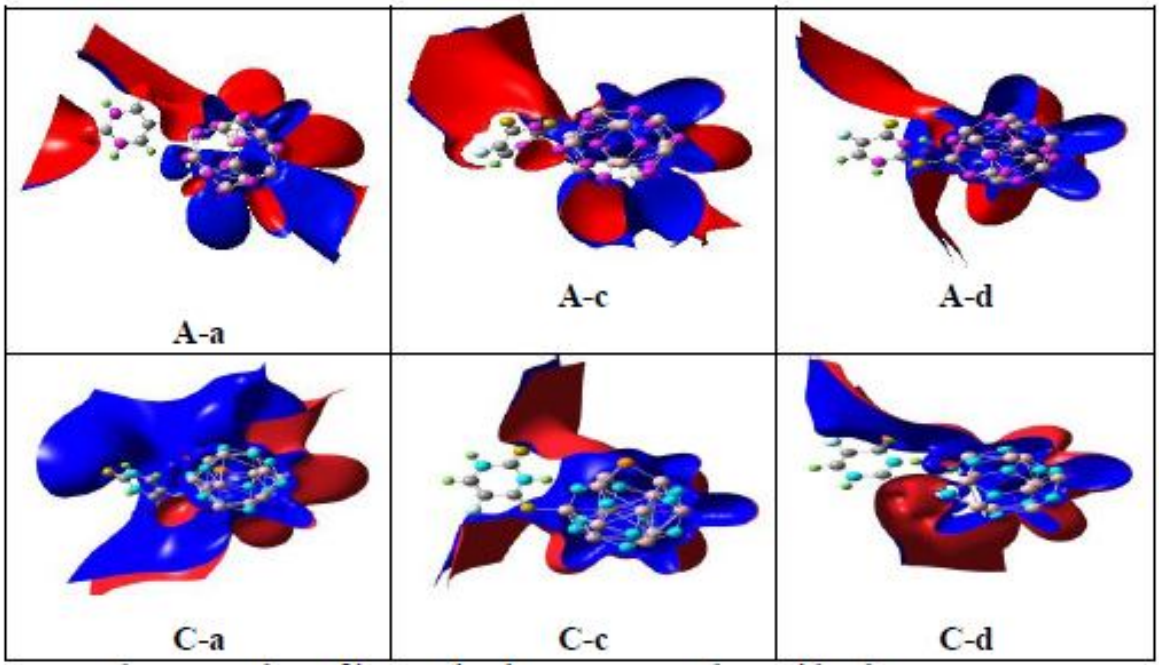

Fig. 7. The MEP plots of interaction between 5-FU drug with Al12N12 nanocage at the A-a to C-d models.

Molecular Electrostatic Potential (MEP) Plots

One of the practical methods to determine the shape, size, charge distributions and nucleophilic or electrophilic of molecule and regions of negative, neutral and positive of the system is molecular electrostatic potential (MEP) [61]. The MEP plots for A-a, A-c, A-d, C-a, C-c and C-d models are calculated and the results are shown in Fig. 7.

In the MEP plots, the blue and red colors represent the positive and negative charges or the nucleophilic and electrophilic regions, respectively. Based on the MEP plots, the most positive density is distributed around 5-FU…AlN nanocage and the most negative density is localized around the 5-FU…AlN surface. The results show that the surface of 5-FU…nanocage is a good position for attacking electrophilic species and the surface of 5-FU…nanocage is suitable for attacking nucleophilic species. These positions are suitable for the interaction of 5-FU drugs with biological cells in body.

Natural Bond Orbital (NBO)

To further understand the interaction 5-FU with the surface of pristine and P doped Al12N12, the natural bond orbital (NBO) parameters are calculated for all the systems. For doing so, the stabilization energy (second-order perturbation energy) $E^{(2)}$ [62] between the bond orbitals (i) and anti-bond orbitals (j) or Rydberg orbitals (j) is calculated:

$$E^{(2)} = q_i \frac{F_{ij}^2}{\varepsilon_j - \varepsilon_i} \tag{10}$$

where q_i , F_{ij} , ε_i and ε_j are the donor occupancy orbital, off-diagonal, and orbital energies (i and j). The calculated results (see Table 4) reveal that the $E^{(2)}$ values for all the systems are in the range of 1.49-19.32 Kcal mol^{-1}.

The highest values of $E^{(2)}$ for the A-a, A-c, A-d, C-a, C-c and C-d models are observed for the electron transition between donor orbital to acceptor orbital in $\pi N3-Al1 \rightarrow \pi^* N4-Al3$. Comparison the results indicate that the $E^{(2)}$ values for the transition in $\pi N3-Al1 \rightarrow \pi^* N4-Al3$ with 19.32 kcal mol^{-1} stabilization energy is more than that in other transitions. The lowest $E^{(2)}$ values for A-a, A-c, A-d, C-a, C-c and C-d models are observed for the electron

Table 4. The Second-order Perturbation Energies (2) (Donor (i) → Acceptor (j)) for A-a to C-d Models

Structure	Donor(i)	→	Acceptor(j)	$E^{(2)}$ (kcal mol^{-1})	E(j)-E(i) (a.u.)	F(i,j) (a.u.)
A-a	σN_4-Al_1	→	$\sigma^* N_2$-Al_1	1.49	0.75	0.030
	σN_1-Al_1	→	$\sigma^* N_6$-Al_5	6.11	0.68	0.058
	πN_3-Al_1	→	$\pi^* N_4$-Al_3	18.16	0.39	0.076
A-c	σN_3-Al_1	→	$\sigma^* N_1$-Al_1	1.93	0.74	0.034
	σN_1-Al_1	→	$\sigma^* N_6$-Al_5	6.26	0.69	0.059
	πN_3-Al_1	→	$\pi^* N_4$-Al_3	18.42	0.40	0.077
A-d	σN_3-Al_1	→	$\sigma^* N_2$-Al_1	1.59	0.76	0.031
	σN_1-Al_1	→	$\sigma^* N_6$-Al_5	6.18	0.68	0.058
	πN^3-Al^1	→	$\pi^* N_4$-Al_3	18.03	0.38	0.075
C-a	σN_3-Al_1	→	$\sigma^* N_3$-Al_5	1.80	0.77	0.033
	σN_1/P-Al_1	→	$\sigma^* N_6$-Al_5	5.27	0.54	0.048
	πN_3-Al_1	→	$\pi^* N_4$-Al_5	17.89	0.39	0.075
C-c	σN_3-Al_1	→	$\sigma^* N_3$-Al_3	1.92	0.68	0.032
	σN_1/P-Al_1	→	$^* N_6$-Al_5	5.39	0.53	0.049
	πN_3-Al_1	→	$\pi^* N_4$- Al_3	19.23	0.41	0.079
C-d	σN_3-Al_1	→	$\sigma^* N_3$-Al_3	2.22	0.78	0.037
	σN_1/P-Al_1	→	$\pi^* N_3$-Al_1	5.41	0.47	0.045
	πN_3-Al_1	→	$\pi^* N_4$- Al_3	17.25	0.38	0.073

transition in $\pi N4-Al1 \rightarrow \pi^* N2-Al1$. According to these results, the stabilization energy $E^{(2)}$ values of pristine models (A-a, A-c, A-d), except C-c models, are more than those of the P-doped nanocage. This result confirms that the interaction of 5-FU with P-doped AlN nanocage is lower than that in pristine AlN nanocage and is in a good agreement with MEP and RDG results.

Infrared (IR) and UV-Vis Spectra

The infrared (IR) spectra for the interaction of 5-FU with the pristine and P-doped AlN nanocage are shown in Fig. S6. Inspection of IR spectra for all the systems indicates the remarkable peaks at 1000, 1600, 2000 and 2600 cm^{-1}, pertaining to the stretching vibrations of O-C, N-C-N, and C≡N bonds, respectively.

The UV-Vis spectra of 5-FU drug adsorption on the pristine and P-doped AlN nanocage are calculated by TD-DFT method and calculated results are given in Table 5 and the UV-Vis spectra are shown in Fig. S7.

The maximum peaks of UV-Vis spectrum at the A-a,

Table 5. The UV-Vis Electron Transient between the Occupied and Unoccupied Orbitals for A-a to C-d Models

Model	Excited state	Wavelength (nm)	Excitation energy (eV)	Configurations composition	F
	$S_0 \rightarrow S_8$	323.11	3.8372	0.6(H-2→L+1) + 0.2(H→L+1)	0.0044
A-a	$S_0 \rightarrow S_{14}$	369.45	3.3559	0.9(H-10→L) + 0.05(H-7→L)	0.0022
	$S_0 \rightarrow S_{20}$	325.21	3.8125	0.024(H-18→L) + 0.93(H-11→L)	0.0061
	$S_0 \rightarrow S_1$	398.08	3.1146	0.9(H→L) + 0.1(H→L+1)	0.0027
A-c	$S_0 \rightarrow S_4$	378.14	3.2788	0.1(H-3→L) + 0.82(H→L+1)	0.0034
	$S_0 \rightarrow S_{19}$	298.49	4.1537	0.6(H-9→L) + 0.24(H-9→L+1)	0.0082
	$S_0 \rightarrow S_5$	350.11	3.5413	0.99(H→L+1)	0.0020
A-d	$S_0 \rightarrow S_{16}$	293.57	4.2233	0.81(H-9→L) + 0.1(H→L+4)	0.0027
	$S_0 \rightarrow S_{18}$	292.31	4.2415	0.03(H-10→L) + 0.933(H→L+2)	0.0128
	$S_0 \rightarrow S_3$	368.93	3.3606	0.14(H-2→L) + 0.64(H-1→L)	0.0106
C-a	$S_0 \rightarrow S_{10}$	388.99	3.1873	0.24(H-9→L) + 0.7(H→L+1)	0.0129
	$S_0 \rightarrow S_{14}$	370.73	3.3443	0.041(H-12→L) + 0.9(H-10→L)	0.0092
	$S_0 \rightarrow S_1$	448.49	2.7645	0.99(H→L)	0.0091
C-c	$S_0 \rightarrow S_{14}$	340.90	3.6369	0.95(H-4→L)	0.0107
	$S_0 \rightarrow S_{22}$	301.13	4.1173	0.98(H-12→L)	0.0197
C-d	$S_0 \rightarrow S_{20}$	292.37	4.2406	0.824(H-1→L+2) + 0.1(H→L+2)	0.0098
	$S_0 \rightarrow S_7$	450.01	2.7552	0.4(H-6→L) + 0.3(H-3→L)	0.0850
	$S_0 \rightarrow S_{14}$	384.33	3.2260	0.424(H-11→L) + 0.21(H-9→L)	0.1804

A-c, A-d, C-a, C-c and C-d models are shown at 325.21, 298.49, 292.31, 388.99, 301.13 and 384.33 nm with oscillator strengths of 0.0061, 0.0082, 0.0128, 0.0129, 0.0197 and 0.1804, respectively. The maximum peaks of all adsorption system are localized in the ultraviolet region, and with doping P atom the wavelength of system increases. On the other hand, the maximum peaks for the A-a, A-c, A-d, C-a, C-c and C-d models occur in transitions of 0.024(H-18→L) + 0.93(H-11→L), 0.6(H-9→L) + 0.24(H-9→L+1), 0.03(H-10→L) + 0.933(H→L+2), 0.24(H-9→L) + 0.7(H→L+1), 0.98(H-12→L), and 0.424(H-11→L) +0.21(H-9→L), respectively.

CONCLUSIONS

Using the DFT and TD-DFT method, the interactions of 5-Fluorouracil drug with the surface of pristine and P-doped Al12N12 nanocage are investigated at the cam-B3LYP/6-31G(d,p) level of theory. The geometrical results reveal that the bond distance and bond angle between 5-FU and AlN nanocage are in the range of 1.90-2.25 Å and 102.41-111.13º, respectively. The values of adsorption energy, enthalpy and Gibbs free energy for the systems understudy are negative and all the adsorption process are exothermic and spontaneous in view of the thermodynamic approach.

The changes of Gibbs free energy in the water and ethanol phase ($\Delta\Delta G(sol)$) for adsorption of the 5-FU drug on the surface AlN nanocage for all systems are positive. The low changes in bandgap energy of the 5-FU/AlN nanocage system indicate that the pristine and P-doped AlN nanocage are not good candidates for making a sensor for the 5-FU drug in a biological system. The AIM results show that the values of $\nabla^2\rho$ and H_{BCP} for all systems are positive and detonate that the interaction between 5-FU and nanocage is electrostatic in nature, and this result is in agreement with RDG and NBO results. The calculated results demonstrated that the AlN nanocage could not be a sensitive sensor for detecting 5-FU, whereas the pristine and P doped Al12N12 nano cage can be used as a carrier of the 5-FU drug in a biological system.

ACKNOWLEDGMENTS

The author thanks the Computational Information Center of Malayer University for providing the necessary facilities to carry out the research.

Supplementary Data

Figures S1- S7 are given in supplementary data.

REFERENCES

[1] Beheshtian, J.; Baei, M. T.; Peyghan, A. A.; Bagheri, Z., Electronic sensor for sulfide dioxide based on AlN nanotubes: a computational study. *J. Mol. Model.* **2012**, *18*, 4547-4750, DOI: 10.1007/s00894-012-1476-2.

[2] Stan, G.; Ciobanu, C.; Thayer, T.; Wang, G.; Creighton, J.; Purushotham, K.; Bendersky, L.; Cook, R., Elastic moduli of faceted aluminum nitride nanotubes measured by contact resonance atomic force microscopy. *Nanotechnology*. **2009**, *20*, 35706-357014, DOI: 10.1088/0957-4484/20/3/035706.

[3] Kakanakova-Georgieva, A.; Gueorguiev, G. K.; Yakimova, R.; Janzen, E., Effect of impurity incorporation on crystallization in AlN sublimation epitaxy, *J. Appl. Phys.* **2004**, *96*, 5293-5297, DOI: 10.1063/1.1785840.

[4] Baei, M. T.; Peyghan, A. A.; Bagheri, Z., Fluorination of the exterior surface of AlN nanotube: a DFT study, *Superlattic. Microst.* **2013**, *53*, 9-15, DOI: 10.1016/j.spmi.2012.09.010.

[5] Nejati, K.; Hosseinian, A.; Vessally, E.; Bekhradnia, A.; Edjlali, L., A comparative DFT study on the interaction of cathinone drug with BN nanotubes, nanocages, and nanosheets. *Appl. Surf. Sci.* **2017**, *422*, 763-768, DOI: 10.1016/j.apsusc.2017.06.082.

[6] Beheshtian, J.; Ahmadi Peyghan, A.; Bagheri, Z., A first-principles study of H_2S adsorption and dissociation on the AlN nanotube. *Physica E.* **2012**, *44*, 1963-1968, DOI: 10.1016/j.physe.2012.06.003.

[7] Samadizadeh, M.; Rastegar, S. F.; Peyghan, A. A., F-, Cl-, Li and Na adsorption on AlN nanotube surface: A DFT study. *Physica E.* **2015**, *69*, 75-80, DOI: 10.1016/j.physe.2015.01.021.

[8] Yakimova, R.; Kakanakova-Georgieva, A.; Yazdi, G. R.; Gueorguiev, G. K.; Syväjärvi, M., Sublimation growth of AlN crystals: growth mode and structure evolution. *J. Cryst. Growth*. **2005**, *281*, 81-86, DOI: 10.1016/j.jcrysgro.2005.03.015.

[9] Ishihara, M.; Manabe, T.; Kumagai, T.; Nakamura, T.; Fujiwara, S.; Ebata, Y.; Shikata, S.; Nakahata, H.; Hachigo, A.; Koga, Y., Synthesis and surface acoustic wave property of aluminum nitride thin films fabricated on silicon and diamond substrates using the sputtering method. *Jap. J. Appl. Phys.,* **2001**, *40*, 5065-5068, DOI: iopscience.iop.org/article/10.1143/JJAP.40.5065.

[10] Wu, Q.; Hu, Z.; Wang, X.; Lu, Y.; Chen, X.; Xu, H.; Chen, Y., Synthesis and characterization of faceted hexagonal aluminum nitride nanotubes. *J. Am. Chem. Soc.* **2003**, *125*, 10176-10177, DOI: org/10.1021/ja0359963.

[11] Wu. Q.; Hu, Z.; Wang, X.; Chen, Y.; Lu, Y., Synthesis and optical characterization of aluminum nitride nanobelts. *J. Phys. Chem. B*. **2003**, *107*, 9726-9729, DOI: org/10.1021/jp035071+.

[12] Tondare, V.; Balasubramanian, C.; Shende, S.; Joag, D.; Godbole, V.; Bhoraskar, S.; Bhadbhade, M., Field emission from open-ended aluminum nitride nanotubes. *Appl. Phys. Lett.* **2002**, *80*, 4813-4815, DOI: abs/10.1063/1.1482137.

[13] Ahmadi, A.; Hadipour, N. L.; Kamfiroozi, M.;

Bagheri, Z., Theoretical study of aluminum nitride nanotubes for chemical sensing of formaldehyde. *Sens. Actuator. B. Inside. Chem.* **2012**, *161*, 1025-1029, DOI: org/10.1016/j.snb.2011.12.001.

[14] Beheshtian, J.; Ahmadi Peyghan, A.; Bagheri, Z., Quantum chemical study of fluorinated AlN nanocage, *Appl. Surf. Sci.* **2012**, *259*, 631-636, DOI: org/10.1016/j.apsusc.2012.07.088.

[15] Rastegar, S. F.; Peyghan, A. A.; Ghenaatian, H. R.; Hadipour, N. L., NO_2 detection by nanosized AlN sheet in the presence of NH_3: DFT studies. *Appl. Surf. Sci.* **2013**, *274*, 217-220, DOI: org/10.1016/j.apsusc.2013.03.019.

[16] Zhang, Y.; Zheng, X.; Zhang, S.; Huang, S.; Wang, P.; Tian, H., Bare and Ni decorated Al12N12 cage for hydrogen storage: a first-principles study. *Int. J. Hydrogen. Energy.* **2012**, *37*, 12411-12419, DOI: org/10.1016/j.ijhydene.2012.06.056.

[17] Shakerzadeh, E.; Barazesh, N.; Zargar Talebi, S., A comparative theoretical study on the structural, electronic and nonlinear optical features of B12N12 and $Al_{12}N_{12}$ nanoclusters with the groups III, IV and V dopants. *Superlat. Microstr.* **2014**, *76*, 264-276, DOI: org/10.1016/j.spmi.2014.09.037.

[18] Niu, M.; Yu, G.; Yang, G.; Chen, W.; Zhao, X.; Huang, X., Doping the alkali atom: an effective strategy to improve the electronic and nonlinear optical properties of the inorganic Al12N12 nanocage. *Inorg. Chem.* **2014**, *53*, 349-358, DOI: org/10.1021/ic4022917.

[19] Fallahi, P.; Jouypazadeh, H.; Farrokhpour, H., Theoretical studies on the potentials of some nanocages (Al12N12, Al12P12, B12N12, Be12O12, C12Si12, $Mg_{12}O_{12}$, and C_{24}) on the detection and adsorption of Tabun molecule: DFT and TD-DFT study. *J. Mol. Liq.* **2018**, *260*: 138-148, DOI: org/10.1016/ j.molliq.2018.03.085.

[20] Esrafili, M. D.; Nurazar, R., Efficient dehydrogenation of formic acid using Al12N12 nanocage: A DFT study. *Superlat. Microstr.* **2014**, *75*, 17-26, DOI: org/10.1016/j.spmi.2014.07.007.

[21] Jouypazadeh, H.; Farrokhpour, H., DFT and TD-DFT study of the adsorption and detection of sulfur mustard chemical warfare agent by the C24, C12Si12, Al12N12, Al12P12, Be12O12, B12N12 and Mg12O12 nanocages. *J. Mol. Str.* **2018**, *1164*, 227-238, DOI: org/10.1016/j.molstruc.2018.03.051.

[22] Azimi, F.; Tazikeh-Lemeski, E., Effects of C_{12} adsorption over the optical and electronic properties of Al12N12 and Al12CN11 fullerenes: Density functional theory study. *Physica E.* **2018**, *103*, 35-45, DOI: org/10.1016/j.physe.2018.05.019.

[23] Solimannejad, M.; Kamalinahad, S.; Shakerzadeh, E., Selective detection of toxic cyanogen gas in the presence of O_2, and H_2O molecules using an AlN nanocluster. *Phys. Lett. A.* **2016**, *380*, 2854-2860, DOI: org/10.1016/j.physleta.2016.06.050.

[24] Shokuhi Rad, A.; Ayub, K., Adsorption properties of acetylene and ethylene molecules onto pristine and nickel-decorated Al12N12 nanoclusters. *Mater. Chem. Phys.* **2017**, *194*, 337-344, DOI: org/10.1016/j.matchemphys.2017.04.002.

[25] Shokuhi Rad, A.; Ayub, K., coordination of nickel atoms with Al12X12 (X = N, P) nanocages enhances H_2 adsorption: a surface study by DFT. *Vacuum.* **2016**, *133*, 70-80, DOI: org/10.1016/j.vacuum.2016.08.017.

[26] Baei, M. T.; Ramezani Taghartapeh, M.; Tazikeh Lemeski, E.; Soltani, A., A computational study of adenine, uracil, and cytosine adsorption upon AlN and BN nanocages. *Physica B.* **2014**, *444*, 6-13, DOI: org/10.1016/j.physb.2014.03.013.

[27] Shokuhi Rad, A., Ayub, K., A comparative density functional theory study of guanine chemisorption on Al12N12, Al12P12, B12N12, and $B_{12}P_{12}$ nano-cages. *J. Alloy. Comp.* **2016**, *672*, 161-169, DOI: org/10.1016/ j.jallcom.2016.02.139.

[28] Zhang, Y.; Zheng, X.; Zhang, S.; Huang, S.; Wang, P.; Tian, H., Bare, and Ni decorated Al12N12 cage for hydrogen storage: a first-principles study. *Int. J. Hydrogen. Energy.* **2012**, *37*, 12411-12419, DOI: org/10.1016/j.ijhydene.2012.06.056.

[29] Beheshtian, J.; Ahmadi Peyghan, A.; Bagheri, Z., Quantum chemical study of fluorinated AlN nanocage. *Appl. Surf. Sci.* **2012**, *259*, 631-636, DOI: org/10.1016/j.apsusc.2012.07.088.

[30] Baei, M. T.; Soltani, A.; Hashemian, S.; Mohammadian, H., Al12N12 nanocage as a potential

sensor for phosgene detection. *Can. J. Chem*. **2014**, *92*, 605-610, Doi/abs/10.1139/cjc-2014-0056#.XgcmzVUzbIU.

[31] Tazikeh-Lemeski, E., Al12CN11 nano-cage sensitive to NH_3 detection: A first-principles study. *J. Mol. Str.* **2017**, *1135*, 166-173, DOI: org/10.1016/ j.molstruc.2017.01.006.

[32] Baei, M. T.; Soltani, A.; Torabi, P.; Hashemian, S., Al12N12 nanocage as potential adsorbent for removal of acetone from environmental systems. *Monatsh. Chem*. **2015**, *146*, 891-896, DOI: 10.1007/s00706-014-1365-8.

[33] Soltani, A.; Ghafouri Raz, S.; Ramezani Taghartapeh, M.; Varasteh Moradi, A.; Zafar Mehrabian, R., *Ab initio* study of the NO_2 and SO_2 adsorption on Al12N12 nano-cage sensitized with gallium and magnesium. *Comp. Mater. Sci.* **2013**, *79*, 795-803, DOI: org/ 10.1016/j.commatsci.2013.07.011.

[34] Shokuhi Rad, A.; Ayub, K., Adsorption of pyrrole on Al12N12, Al12P12, B12N12 and B12P12 fullerene-like nano-cages; a first-principles study. *Vacuum*. **2016**, *13*, 135-141, DOI: org/ 10.1016/j.vacuum.2016.06.012.

[35] Baei, M. T.; Tazikeh Lemeski, E.; Soltani, A., DFT study of the adsorption of H_2O_2 inside and outside Al12N12 nano-cage, *Russian. J. Phys. Chem. A*. **2017**, *91*, 1527-1534, DOI: 10.1134/ S0036024417080210.

[36] Longley, D. B.; Harkin, D. P.; Johnston, P. G., 5-fluorouracil: Mechanisms of action and clinical strategies. *Nat. Rev. Cancer*. **2003**, *3*, 330-338, DOI: articles/nrc1074.

[37] Nunes, J. H. B.; Bergamini, F. R. G.; Lustri, W. R.; de Paiva, P. P.; Ruiz, A. L. T. G.; de Carvalho, J. E.; Corbi, P. P., Synthesis, characterization and *in vitro* biological assays of A silver(I) complex with 5-fluorouracil: A strategy to overcome multidrug-resistant tumor cells. *J. Fluor. Chem*. **2017**, *195*, 93-101, DOI: org/10.1016/j.jfluchem.2017.01.016.

[38] Thoppil, A. A.; Choudhary, S.; Kishore, N., Competitive binding of anticancer drugs 5-fluorouracil and cyclophosphamide with serum albumin: calorimetric insights. *Biochim. Biophys. Acta. Gen. Subj.* **2016**, *1860*, 917-929.

[39] Arias, J. L., Novel strategies to improve the anticancer action of 5-fluorouracil by using drug delivery systems. *Molecules*. **2008**, *13*, 2340-2369, DOI: org/ 10.3390/molecules13102340.

[40] Luo, H.; Ji, D.; Li, C.; Zhu, Y.; Xiong, G.; Wan, Y., Layered nanohydroxyapatite as a novel nanocarrier for controlled delivery of 5-fluorouracil. *Int. J. Pharm*. **2016**, *513*, 17-25, DOI: org/10.1016/ j.ijpharm.2016.09.004.

[41] Pan, G.; Jia, Tt.; Huang, Qx.; Qiu, Yy.; Xu, J.; Yin, Ph.; Liu, T., Mesoporous silica nanoparticles (MSNs)-based organic/inorganic hybrid nanocarriers loading 5-Fluorouracil for the treatment of colon cancer with improved anticancer efficacy. Colloids. *Surf. B*. **2017**, *159*, 375-385, DOI: 10.1016/ j.colsurfb.2017.08.013.

[42] Egodawatte, S.; Dominguez, S.; Larsen, Sc., Solvent effects in the development of a drug delivery system for 5-fluorouracil using magnetic mesoporous silica nanoparticles. *Microporous. Mesoporous. Mater*. **2017**, *237*, 108-116, DOI: 10.1016/ j.micromeso.2016.09.024.

[43] Zhu, K.; Ye, T.; Liu, J.; Peng, Z.; Xu, S.; Lei, J.; Deng, H.; Li, B., Nanogels fabricated by lysozyme and sodium carboxymethyl cellulose for 5-fluorouracil controlled release. *Int. J. Pharm*. **2013**, *441*, 721-727, DOI: 10.1016/j.ijpharm.2012.10.022.

[44] Yang, H. C.; Hon, M. H., The effect of the molecular weight of chitosan nanoparticles and its application on drug delivery. *Microchem. J.* **2009**, *92*, 87-91, DOI: 10.1016/j.microc.2009.02.001.

[45] Lakkakula, J. R.; Matshaya, T.; Krause, R. W. M., Cationic cyclodextrin/alginate chitosan nanoflowers as 5-fluorouracil drug delivery system. *Mater. Sci. Eng. C*. **2017**, *70*, 169-177, DOI: 10.1016/ j.msec.2016.08.073.

[46] Ehi-Eromosele C. O.; Ita, B. I.; Iweala, E. E. J., Silica coated LSMO magnetic nanoparticles for the pH-Responsive delivery of 5-Fluorouracil anticancer drug. *Colloids. Surf. A*. **2017**, *530*, 164-171, DOI: 10.1016/j.colsurfa.2017.07.059.

[47] Vatanparast, M.; Shariatinia, Z., AlN and AlP doped graphene quantum dots as novel drug delivery systems for 5-fluorouracil drug: Theoretical studies. *J. Fluorine. Chem*. **2018**, *211*, 81-93, DOI: 10.1016/ j.jfluchem.2018.04.003.

[48] Hazrati, K.; Hadipour, N. L., Adsorption behavior of 5-fluorouracil on pristine, B-, Si- and Al-doped C60 fullerenes: A first-principles study. *Physics. Lett. A*. **2016**, *380*, 937-941, DOI: 10.1016/j.physleta.2016.01.020.

[49] Shayan, K.; Nowroozi, A., Boron nitride nanotubes for delivery of 5-fluorouracil as anticancer drug: a theoretical study. *Appl. Surf. Sci.* **2018**, *428*, 500-513, DOI: 10.1016/j.apsusc.2017.09.121.

[50] Rezaei-Sameti, M.; Javadi Jukar, N., A computational study of nitramide adsorption on the electrical properties of pristine and C-replaced boron nitride nanosheet, *J. Nanostruct. Chem.* **2017**, *7*, 293-307, DOI: 10.1007/s40097-017-0237-2.

[51] Rezaei‑Sameti, M.; Moradi, F., Interaction of isoniazid drug with the pristine and Ni-doped of 4) armchair GaNNTs: A first principle study, *J. Incl. Phenom. Macrocycl. Chem.* **2017**, *88*, 209-218, DOI: 10.1007/s10847-017-0720-x.

[52] Rezaei-Sameti, M.; Bagheri, M., Interaction of SO_2 gas with the pristine and B & O atoms doped AlNNTs: A DFT study. *J. Phys. Theo. Chem.* **2017**, *14*, 63-80, DOI: jptc.srbiau.ac.ir/article_10955.

[53] Rezaei-Sameti, M.; Behbahani, H. J., Interaction of HCN molecule with the pristine and Al, S and Al & S doped beryllium oxide nanotube: A computational study. *Phys. Chem. Res.* **2018**, *6*, 31-43, DOI: 10.22036/pcr.2017.89007.1388.

[54] Rezaei‑Sameti, M.; Zarei, P., NBO, AIM, HOMO-LUMO and thermodynamic investigation of the nitrate ion adsorption on the surface of pristine, Al and Ga doped BNNTs: A DFT study, *Adsorption,* **2018**, *24*, 757-767, DOI: 10.1007/s10450-018-9977-7.

[55] Rakhshi, M.; Mohsennia, M.; Rasa, H.; Rezaei Sameti, M., First-principle study of ammonia molecules adsorption on boron nitride nanotubes in presence and absence of static electric field and ion field. *Vacuum*. **2018**, *155*, 456-464, DOI: 10.1016/j.vacuum.2018.06.047.

[56] Yanai, T.; PTew, D.; CHandy, N., A new hybrid exchange-correlation functional using the Coulomb-attenuating method (CAM-B3LYP), *Chem. Phys. Let.* **2004**, *393*, 51-57, DOI: 10.1016/j.cplett.2004.06.011.

[57] Schmidt, M. W.; Baldridge, K. K.; Boatz, J. A.; Elbert, S. T.; Gordon, M. S.; Jensen, J. H.; Koseki, S.; Matsunaga, N.; Nguyen, K. A.; Su, S. J.; Windus, T. L.; Dupuis, M.; Montgomery, J. A., General atomic and molecular electronic structure system. *J. Comp. Chem.* **1993**, *14*, 1347-1363, DOI: 10.1002/jcc.540141112.

[58] Bader, R. F. W., Atoms in Molecules: A Quantum Theory, Oxford University Press, Oxford, 1990.

[59] Johnson, E. R.; Keinan, S.; Mori-Sanchez, P.; Contreras-Garcia, J.; Cohen, A. J.; Yang, W., *J. Am. Chem. Soc.* **2010**, *132*, 6498-6506, DOI: 10.1021/ja100936w.

[60] Bulat, F. A.; Toro-Labbé, A.; Brinck, T.; Murray, J. S.; Politzer, P., Quantitative analysis of molecular surfaces: areas, volumes, electrostatic potentials and average local ionization energies. *J. Mol. Model.* **2010**, *16*, 1679-1691, DOI: 10.1007/s00894-010-0692-x.

[61] Bulat, F. A.; Burgess, J. S.; Matis, B. R.; Baldwin, J. W.; Macaveiu, L.; Murray, J. S.; Politzer, P., Hydrogenation and fluorination of graphene models: analysis via the average local ionization energy. *J. Phys. Chem. A*. **2012**, *116*, 8644-8652, DOI: 10.1021/jp3053604.

[62] Glendening, E.; Reed, A.; Carpenter, J.; Weinhold, F., NBO Version 3.1, GaussianInc., Pittsburg, PA, CT, 2003.